

## Optical and Structural Studies of Mn<sup>2+</sup> Doped SbPO<sub>4</sub>-ZnO-PbO Glasses

Renata S. Manzan,<sup>a,b</sup> José P. Donoso,<sup>c</sup> Claudio J. Magon,<sup>c</sup> Igor d'Anciães A. Silva,<sup>c</sup>  
Christian Rüssel<sup>d</sup> and Marcelo Nalin<sup>\*a</sup>

<sup>a</sup>Laboratório de Vidros Especiais (LAViE), Instituto de Química, Universidade Estadual Paulista  
"Júlio de Mesquita Filho" (Unesp), 14800-060 Araraquara-SP, Brazil

<sup>b</sup>Departamento de Química, Universidade Federal de São Carlos (UFSCar), CP 676,  
13565-905 São Carlos-SP, Brazil

<sup>c</sup>Instituto de Física de São Carlos, Universidade de São Paulo (USP),  
13566-590 São Carlos-SP, Brazil

<sup>d</sup>Otto Schott Institute of Materials Research, Friedrich Schiller University of Jena,  
D-07743 Jena, Germany

New glass compositions in the system 1 - x(SbPO<sub>4</sub>-ZnO-PbO)-xMnO (with 0 ≤ x ≤ 20 in mol%) were prepared by melt-quenching methodology. Thermal, structural and optical properties of the new glasses were systematically studied by means of differential scanning calorimetry (DSC), UV-Vis and Raman spectroscopy, fluorescence and electronic paramagnetic resonance (EPR). The addition of MnO increases the thermal stability of the glasses with Tx - Tg close to 140 °C for higher Mn contents. EPR measurements show that Mn<sup>2+</sup> ions are in octahedral arrangement which is in agreement with UV-Vis and luminescence results. Samples present red luminescence when excited with 408 nm source.

**Keywords:** antimony glasses, manganese, luminescence, structure

### Introduction

Special glasses containing transition metal (TM) ions have aroused the interest of researchers around the globe during the last years to explore an amount of interesting phenomena like luminescence,<sup>1-3</sup> non-linear<sup>4,5</sup> and, more recently, magnetic properties.<sup>6-8</sup>

The interest in luminescent glasses, mainly those containing Mn<sup>2+</sup> ions, arises from the fact that, depending on the composition of the glass host, the material can be used as a phosphor with emission range from green to red.<sup>3</sup> However, it must be taken into account that the luminescent behavior is strongly dependent on the surroundings of the Mn<sup>2+</sup> ions, and depending on the composition it can even be completely suppressed.<sup>9</sup>

It is known that crystals present better luminescent properties than glasses (i.e., higher life times and narrow emission bands), so, to enhance the optical properties, including preparing better phosphors, an alternative is

to crystallize the glass host in order to obtain a glass-ceramic, where the transition metal should be present in the crystalline phase. In multi-component glass systems it is not that trivial because a lot of different and undesired phases can rise up during the thermal treatment. Thus, the control of the crystallization process and the knowledge of the environment of the TM are essential to maximize the efficiency of the phosphor.

Structural modifications of the local environment of the TM ion incorporated into the network resulting from thermal treatment or by varying the composition of a glass can be reflected in the electron paramagnetic resonance (EPR) and optical absorption spectra of the TM ions.<sup>10,11</sup> Among the TM ions, Mn<sup>2+</sup> is important because of the extreme sensitivity of its optical and EPR spectra on the nature of the host matrix, and has been frequently used as paramagnetic probes in vitreous systems.<sup>12-16</sup> In glass matrices, manganese may be present as Mn<sup>3+</sup> or Mn<sup>2+</sup> ions, occupying tetrahedral or octahedral site symmetries.<sup>11,17,18</sup> EPR spectroscopy is a particularly suitable technique for the study of local coordination of

\*e-mail: mnalin@iq.unesp.br

Mn<sup>2+</sup> and Mn<sup>4+</sup> ions in glass matrices. In particular, EPR techniques have been extensively used to monitor changes at the manganese sites during crystallization process and to identify spectroscopically distinct manganese sites in glasses.<sup>9,11,12,14,16,19-21</sup>

In such context, the aim of this paper was to study the optical and structural properties of phosphate glasses and glass-ceramics doped with manganese. The samples were studied by thermal analysis, Raman, UV-Vis, EPR and luminescence spectroscopy.

## Experimental

The glass samples were prepared by melt quenching method, in platinum crucible, using SbPO<sub>4</sub>, ZnO, PbO and MnCl<sub>2</sub>·4H<sub>2</sub>O as raw materials. SbPO<sub>4</sub> was previously synthesized as described by Nalin *et al.*<sup>22</sup> The glass composition (100 - x)70SbPO<sub>4</sub>-10ZnO-20PbO-xMnO was chosen to be studied, with x ranging from 0 to 20 mol% as shown in Table 1.

Thermal analyses were performed with a Netsch DSC 404 Pegasus, in nitrogen atmosphere. Small pieces of glass were put in platinum crucibles and analyzed in the range from 25 to 700 °C with a heating rate of 10 °C min<sup>-1</sup>. The characteristic temperatures of the glasses were determined: glass transition (T<sub>g</sub>), onset of crystallization (T<sub>x</sub>) and maximum of crystallization (T<sub>p</sub>). The stability parameter (T<sub>x</sub> - T<sub>g</sub>) was used to estimate the stability of the glass compositions against devitrification. The errors associated with determinations of the temperatures are ± 2 °C for T<sub>g</sub> and T<sub>x</sub> and ± 1 °C for T<sub>p</sub>.

A LabRAM (Jobin Yvon) spectrometer equipped with a micro-Raman microscope was used to obtain the Raman spectra in the range from 100 to 2000 cm<sup>-1</sup>. The spectra were obtained from the polished surface of the glasses. The wavelength of the laser used in measurements was 632.8 nm and the spectral resolution was 4 cm<sup>-1</sup>.

X-Band continuous-wave electron paramagnetic resonance (CW-EPR) spectra were recorded at 50 K on a

Bruker Elexsys E580 spectrometer operating at 9.478 GHz and equipped with an Oxford continuous flow liquid helium cryogenic system. Solid state powder EPR spectra were simulated using the software EasySpin,<sup>23</sup> implemented in MATLAB (MathWorks, Inc.).

Excitation and emission spectra were obtained using a Fluorolog (Horiba Jobin Yvon) equipment at room temperature. Both measurements were obtained from glass pieces. For excitation measurements the emission wavelength was set at 610 nm for samples 05Mn, 3Mn, 5Mn and 10Mn and 650 nm for sample 20Mn. The emission spectra were obtained by exciting at 411 nm.

Since T<sub>g</sub> and T<sub>x</sub> were known, heat treatments were performed between those temperatures in order to control the formation of glass-ceramics, and the absorption spectra were monitored during the heating process in an oven coupled to a Varian Cary 5000 UV-Vis-near infrared (NIR) spectrophotometer in the range from 350 to 800 nm. The spectral resolution was 4 nm.

## Results and Discussion

Antimony based heavy metal oxides glasses present several interesting technological characteristics, concerning their high refractive index,<sup>24</sup> good thermal stability,<sup>25</sup> and good non-linear properties,<sup>26</sup> making them promising materials for photonic applications. However, from the luminescent point of view, such materials were not yet explored. In this sense, this work aimed to study the structural and optical properties of antimony based glasses and glass-ceramics doped with Mn<sup>2+</sup> and the luminescent dependency on the manganese content.

Glasses in the system 100 - x(70SbPO<sub>4</sub>-10ZnO-20PbO)-xMnO (with 0.5 ≤ x ≤ 20, in mol%) were synthesized. The prepared samples were pale yellow, and presented a slight intensification of the color as more manganese was added.

The thermal analyses results are shown in Figure 1a, from which we note an enlargement of the crystallization

**Table 1.** Glass compositions, characteristic temperatures and the stability parameter of the glasses containing different MnO contents

Sample	Glass composition / mol%				Characteristic temperatures / °C		
	SbPO <sub>4</sub>	ZnO	PbO	MnO	T <sub>g</sub>	T <sub>x</sub>	ΔT
0Mn	70	10	20	0	375	482	107
05Mn	70	10	20	0.5	376	482	106
3Mn	70	10	20	3	377	491	114
5Mn	70	10	20	5	379	505	126
10Mn	70	10	20	10	387	522	135
20Mn	70	10	20	20	399	541	142

T<sub>g</sub>: Glass transition temperature; T<sub>x</sub>: crystallization onset temperature; ΔT = T<sub>x</sub> - T<sub>g</sub>.

peak with increase of the manganese content. The characteristic temperatures also increase with the MnO concentration. Since Tx increase is more significant than that of Tg, the thermal stability also rises with increase of manganese content, which may indicate that the Mn<sup>2+</sup> ions favor the disorganization of the glass network making it more difficult to crystallize the glass matrices.

All the thermal results, along with the glass compositions, are summarized in Table 1. The evolution in the characteristic temperatures of the glasses is better observed in Figure 1b, for Tg, Figure 1c for Tx and Figure 1d for the stability parameter.

Raman spectra seen in Figure 2 show the characteristic profile bands of a SbPO<sub>4</sub> based glass.<sup>22</sup> Bands at 1140 and 978 cm<sup>-1</sup> are assigned to  $\nu_{as}$  PO<sub>4</sub> and  $\nu_s$  PO<sub>4</sub>, respectively. Those at 620, 548, 467 and 404 cm<sup>-1</sup> may be attributed to  $\nu_{as}$  P–O–Sb,  $\nu_{as}$  Sb–O,  $\delta_s$  PO<sub>4</sub> and  $\delta_{as}$  Sb–O, respectively.

Those appearing at 204 and 300 cm<sup>-1</sup> were assigned to group modes.<sup>22</sup> From Raman results it was not possible to observe any significant change in the structural arrangement of the glasses despite the low intensity band appearing close 850 cm<sup>-1</sup> for samples containing 5, 10 and 20 mol% of MnO. Such band corresponds to luminescence of Mn<sup>2+</sup> ions present in octahedral sites. If converted to wavelengths, 850 cm<sup>-1</sup> corresponds to 668 nm and can be assigned to transition  ${}^4T_1(G) \rightarrow {}^6A_1(S)$ .<sup>3</sup> Also, it is clear that by increasing the amount of manganese a large luminescent band rises up in the higher energy side and as manganese content increases, the luminescence signal of manganese begins to overlap the band at 1100 nm.

In order to investigate the role of manganese in the structure of the glasses, EPR measurements were done. Figure 3a shows the X-band CW-EPR spectrum measured at 50 K of the 100 – x(70SbPO<sub>4</sub> - 10ZnO - 20PbO) - xMnO

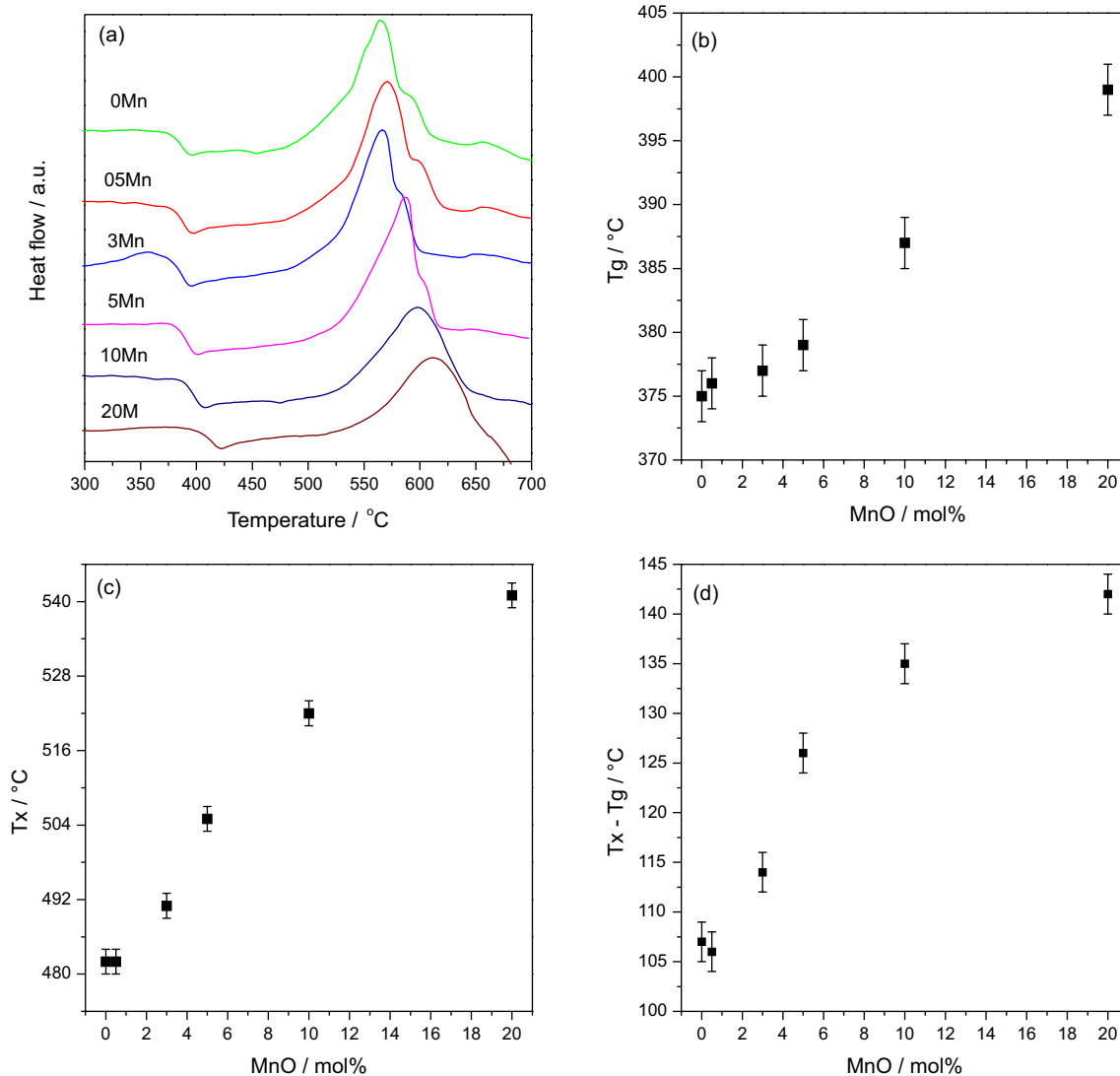


**Figure 1.** (a) Thermal analyses of the glasses with different contents of Mn<sup>2+</sup>. Evolution of the characteristic temperatures of (b) Tg, (c) Tx and (d) thermal stability of the samples.

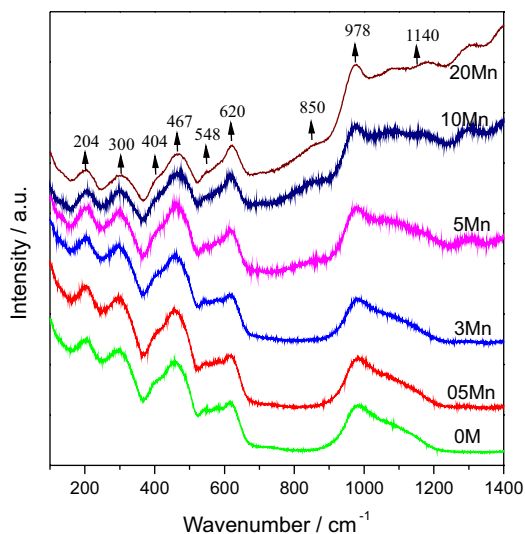


**Figure 2.** Raman spectra of the glasses containing different contents of MnO.

glasses. Two prominent features with effective  $g$ -values of  $g$  ca. 2.0 (around 3300 G) and  $g$  ca. 4.3 (around 1500 G) appeared in all spectra. The former signal, which has been frequently reported in oxide glasses, is attributed to magnetically isolated Mn<sup>2+</sup> ions in symmetry close to octahedral or undistorted cubic sites.<sup>11,27-29</sup> The low field signal at  $g$  ca. 4.3 is associated with isolated Mn<sup>2+</sup> ions in rhombic distorted sites subjected to high crystal field effects.<sup>11,15,18,30,31</sup>

The Mn<sup>2+</sup> ion has a 3d<sup>5</sup> electronic configuration, spin  $S = 5/2$  and ground state <sup>6</sup>S<sub>5/2</sub> (high spin configuration). For d<sup>5</sup> transition metal ions the axial or tetragonal distortion of octahedral crystal field gives rise to three Kramer's doublets,  $\pm 5/2$ ,  $\pm 3/2$  and  $\pm 1/2$ .<sup>32</sup> Application of magnetic field lifts the spin degeneracy of the Kramer's doublets and the resonances observed in the EPR spectra are due to transitions within the Kramer's doublets. The resonance at  $g$  ca. 4.3 is believed to arise from transitions between energy levels of the  $\pm 3/2$  Kramer doublet whereas those at  $g$  ca. 2 arise from transition within the  $\pm 1/2$  Kramer doublet.<sup>12,29,33,34</sup> Manganese has a stable isotope with non-zero nuclear spin, <sup>55</sup>Mn, with  $I = 5/2$  (100% natural abundance), therefore the EPR spectra of Mn<sup>2+</sup> ions at low manganese concentration has a characteristic hyperfine structure composed of six lines, resulting from the dipole-dipole interaction between the magnetic moment of the <sup>55</sup>Mn nuclei and the electronic moment of the paramagnetic Mn<sup>2+</sup> ion. The hyperfine sextet has long been recognized as the main signature of Mn<sup>2+</sup> in glasses.<sup>20</sup>

As can be seen in Figure 3a, the shape of the EPR spectra strongly depends on the MnO content of the glass samples. The EPR spectrum of the sample with lower MnO content ( $x = 0.5$  mol%), exhibits a well-defined isotropic sextet

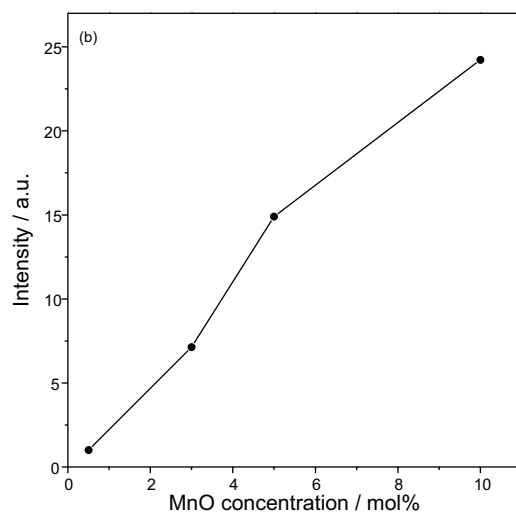
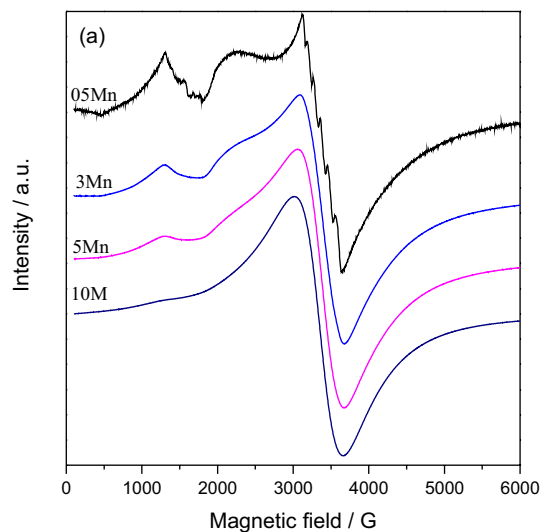


**Figure 3.** (a) EPR spectra of the glasses containing different contents of MnO. (b) Manganese concentration dependence on the EPR line intensity.

centered at  $g$  ca. 2.0, superimposed on a broader background. The hyperfine structure is only barely discernible in the low field resonance at  $g$  ca. 4.3. It should be noted that the signal at  $g$  ca. 4.3 may also have a contribution of natural iron impurity presented in the raw materials. The Fe<sup>3+</sup> ion has also a 3d<sup>5</sup> electronic configuration and the  $g$  ca. 4.3 signal is due to isolated Fe<sup>3+</sup> ions in tetrahedral or octahedral symmetry with rhombic distortion.<sup>20,35,36</sup> When the concentration of manganese increased beyond 1 mol% MnO in the glass samples, the hyperfine structure disappears and the spectra reduces to a broad resonance line centered at  $g$  ca. 2.0 (Figure 3a). The disappearance of the hyperfine structure in glasses with higher content of MnO indicates the increase of dipole-dipole interactions and, at higher MnO concentrations, the presence of magnetic exchange interaction.<sup>16,37,38</sup> The manganese concentration dependence of the EPR line intensity, shown in Figure 3b, was obtained from the double integration of the resonance

line at  $g$  ca. 2.0 and normalized by their mass. The intensity of the resonance at  $g$  ca. 2.0 increases almost linearly with the manganese ions content in the glass up to 10 mol%. This behavior is in agreement with those observed in other manganese doped phosphate glasses.<sup>11,16,29,39</sup>

The resonance signal centered at  $g$  ca. 2.0 is dominant in the  $Mn^{2+}$  spectra of the glass sample with 0.5 mol% of MnO (Figure 3a). For most of the reported EPR studies in manganese-doped glasses, the signal at  $g$  ca. 4.3 is weak if compared to the main resonance at  $g$  ca. 2.0. This result suggests that for low MnO concentration, the  $Mn^{2+}$  ions enter in the  $70SbPO_4-10ZnO-20PbO$  glass as isolated ions occupying predominantly highly ordered environment close to octahedral symmetry, giving the  $g$  ca. 2.0 resonance signal.<sup>11,16,18,38</sup> On the other hand, it should be noted that dominant  $Mn^{2+}$  resonance signal at  $g$  ca. 4.3 has been reported on glasses based on  $B_2O_3-Bi_2O_3$ <sup>15,35</sup> and  $90PbGeO_3-10SbPO_4$ ,<sup>9</sup> indicating that a significant fraction of  $Mn^{2+}$  ions in these glasses are in rhombically octahedral distorted sites.

It is interesting to note the shift of the EPR resonance toward lower magnetic field with increasing MnO content in Figure 3a. For low MnO levels, the  $g$ -value ( $g = 2.005$  for sample with 0.5 and 3 mol% of MnO) is close to the free electron value ( $g_e = 2.0023$ ). At higher MnO concentrations the  $g$ -value shifts to 2.022 (sample 5Mn) and 2.037 (sample 10Mn). Similar changes in  $g$ -values were reported in  $xMnO-(1-x)(Sr-O-P_2O_5)$ <sup>40</sup> and  $Mn_xSr_{1-x}(PO_3)_2$  glasses,<sup>11</sup> where the parameter increased from  $g = 2.00$  for  $x = 0.1$  to  $g = 2.04$  for  $x = 1.0$ . Similar trends were observed in  $LiI-AgI-B_2O_3-MnO$  glasses, where the  $g$ -value increased from 2.0027 to 2.0070 when the MnO content increased from 0.1 to 0.8 mol%.<sup>18</sup> The shift in  $g$ -value with the manganese concentration has been correlated with the bonding character of the  $Mn^{2+}$  ion incorporated in the glass. Values above the free electron  $g$ -value are indicative of more covalent, and those below are related to more ionic  $Mn^{2+}$  bonding character.<sup>11,40</sup> Accordingly, the positive deviation of the  $g$ -value with the MnO content observed in Figure 3 suggests a more covalent character in  $Mn^{2+}$  site for higher Mn content in the  $SbPO_4-ZnO-PbO$  glasses studied here.

The influence of the MnO content on the optical properties of the glasses was investigated by UV-Vis spectroscopy and the absorption spectra may be observed in Figure 4. Results show a sharp band at 411 nm, which is more intense as the manganese content in the glass sample increases. Such band is assigned to  ${}^6A_1(S) \rightarrow {}^4A_1, {}^4E(G)$  from  $Mn^{2+}$  ions in octahedral symmetry which is in agreement with EPR results. This band presents a shoulder around 420 nm which has been assigned to  ${}^6A_1(S) \rightarrow {}^4T_2(G)$  transition. A second band, which is broader, is observed

at about 520 nm only for sample 20Mn and attributed to transition  ${}^6A_1(S) \rightarrow {}^4T_1(G)$ . Considering the presence of such band for the sample more concentrated in MnO, we can rule out the presence of small amounts of  $Mn^{3+}$  ions. In a very detailed study, Konidakis *et al.*<sup>40</sup> showed that even concentrations below 0.07% in  $Mn^{3+}$  ions are enough to present absorption band in this region. Such results are also in agreement with previously reported data.<sup>3</sup>

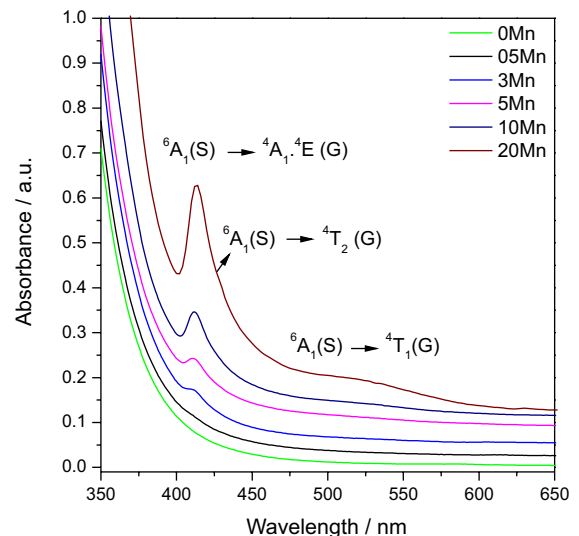


**Figure 4.** Absorption spectra of the glasses with different contents of MnO.

Due to very low concentration and because  $Mn^{3+}$  is silent to EPR measurements, the presence of such ion is difficult to be characterized in glasses.

The red shift observed in the cutting edge as the sample is more concentrated in manganese may be assigned to both charge-transfer excitations from oxygen to  $Mn^{2+}$  and/or  $Mn^{3+}$  and intervalence charge-transfer excitations from  $Mn^{2+}$  towards  $Mn^{3+}$ .<sup>40</sup>

The glasses were studied by luminescence spectroscopy and the results are shown in Figure 5. In the excitation spectra of the glasses, shown in Figure 5a, the absorption profiles are similar to those observed by Winterstein *et al.*<sup>41</sup> The inset in Figure 5a shows a deconvolution of the bands for sample 20Mn. The six d-d transitions were assigned and correspond to transitions from the fundamental level  ${}^6A_1$  of  $Mn^{2+}$  towards the excited states  ${}^4E({}^4D)$ ,  ${}^4T_2({}^4D)$ ,  ${}^4E({}^4G)$ ,  ${}^4A_1({}^4G)$ ,  ${}^4T_2({}^4G)$  and  ${}^4T_1({}^4G)$ , respectively.

Emission spectra of the samples are shown in Figure 5b. Broad bands are observed in the region between 620 and 680 nm, and have a red shift as the concentration increases.  $Mn^{2+}$  ( $d^5$ ) in octahedral symmetry and high spin configuration is not supposed to present allowed transitions. However, if some symmetry distortion is observed the transition become allowed by the Laporte rule and the

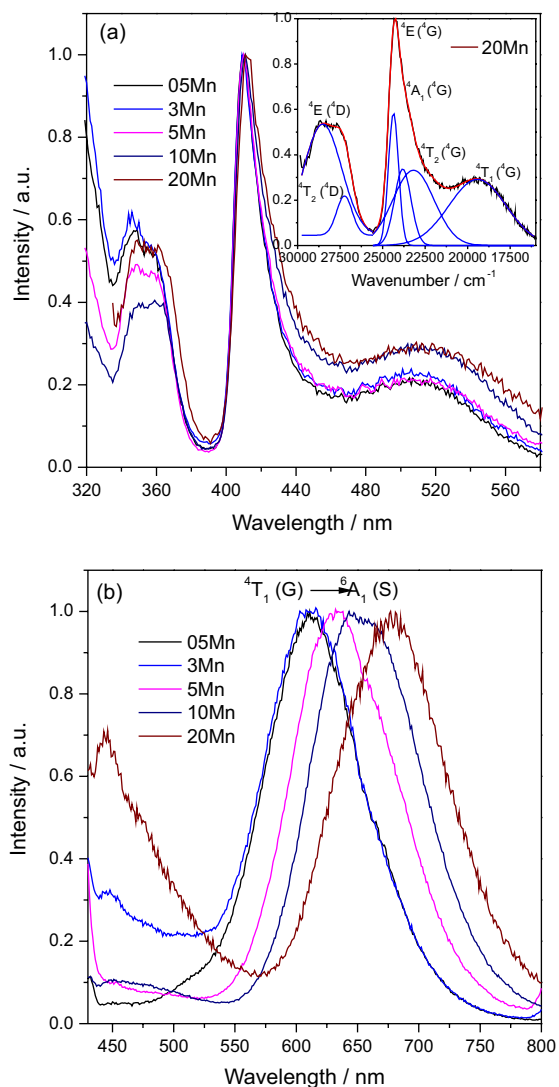


**Figure 5.** (a) Excitation spectra of the samples. The inset shows the deconvolution of the excitation spectra, here represented by sample 20Mn. (b) Emission spectra of the glasses.

emission band can be observed.<sup>42</sup> Usually, if Mn<sup>2+</sup> ions are in tetrahedral arrangement, the emission band appears in the green region while octahedrally surrounded Mn<sup>2+</sup> presents emission from orange to red.<sup>41,43</sup> Following the same argument discussed above, the emission bands shown in Figure 5b were assigned to transition  ${}^4T_1(G) \rightarrow {}^6A_1(S)$  of Mn<sup>2+</sup> in octahedral environment.<sup>42,44</sup> The red shift was already observed by Reisfeld *et al.*<sup>45</sup> and is an indicative that the increase of manganese concentration increases the crystal field strength.

The photograph of the sample without MnO and the sample containing 10 mol% Mn (10Mn) under white light irradiation is shown in Figure 6a. It is clear that the addition of manganese leads to a slight change in the color of the mother glass. This color comes mainly as a result of the absorption band at 410 nm, as observed in Figure 4.

Under excitation of a light source at 480 nm it is possible to observe the red emission of the sample 10Mn while the non-doped sample remains unchanged. The emission lifetime was measured for all samples and the results are summarized in Table 2.

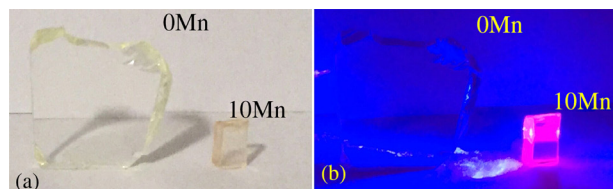


**Figure 6.** (a) Photograph under white light of the glass matrix containing 0 and 10 mol% of MnO; (b) photograph of both samples under illumination of a  $\lambda = 408$  nm light source.

**Table 2.** Lifetime of the emission in the red for the samples containing different amounts of MnO.

Sample	$\tau$ / ms	R <sup>2</sup>
05Mn	$5.65 \pm 0.24$	0.95
3Mn	$5.71 \pm 0.77$	0.99
5Mn	$4.59 \pm 0.54$	0.99
10Mn	$2.66 \pm 0.27$	0.99
20Mn	$0.35 \pm 0.27$	0.99

$\tau$ : Emission lifetime; R<sup>2</sup>: coefficient of determination.

From the results listed in Table 2 it is possible to infer that the lifetimes ( $\tau$ ) are low, but coherent with amorphous materials; increasing the MnO content a decrease in  $\tau$  was also observed, which is in agreement with other results shown by Reisfeld *et al.*<sup>45</sup> Such effect is assigned to luminescence-quenching as a function of the MnO concentration for samples.<sup>3,46</sup>

Nowadays, the preparation of glass-ceramics using such glasses are under investigation in our laboratories in order to obtain longer lifetimes and also focusing on the magnetic properties of such new materials, since the crystallization of MnO in nanoscale from the glass can be achieved by controlled thermal annealing.

## Conclusions

The local symmetry of Mn<sup>2+</sup> in the matrix must be predominantly octahedral, as observed from the results of absorbance spectroscopy, EPR and luminescence.

From thermal analysis results we conclude that the devitrification of glasses becomes less favorable when the manganese concentration increases in the glass composition. This may be an indicative that the ions favor the disorder of the matrix, possibly occupying the interstices. On the other hand, when the concentration of

MnO is higher than 5 mol%, a new band at ca. 850 nm appears in the Raman spectra; however, it corresponds to luminescence of Mn<sup>2+</sup> in Oh symmetry.

The samples containing Mn<sup>2+</sup> ions are luminescent and present red emission when excited with  $\lambda = 408$  nm. The emission band shifts to higher wavelengths along with the Mn content.

## Acknowledgements

The authors are grateful to grants No. 2012/05087-4 and No. 2013/07793-6, São Paulo Research Foundation (FAPESP) for financial support.

## References

- Katayama, Y.; Ueda, J.; Tanabe, S.; *Opt. Mater. Express* **2014**, *4*, 613.
- Song, E.; Zhao, W.; Dou, X.; Zhu, Y.; Yi, S.; Min, H.; *J. Lumin.* **2012**, *132*, 1462.
- Da, N.; Peng, M.; Krolikowski, S.; Wondraczek, L.; *Opt. Express* **2010**, *18*, 2549.
- Schmidt, M. A.; Wondraczek, L.; Lee, H. W.; Granzow, N.; Da, N.; Russell, P. S. J.; *Adv. Mater.* **2011**, *23*, 3681.
- Satyanarayana, T.; Valente, M. A.; Nagarjuna, G.; Veeraiiah, N.; *J. Phys. Chem. Solids* **2013**, *7*, 229.
- Raghuwanshi, V. S.; Harizanova, R.; Haas, S.; Tatchev, D.; Gugov, I.; Dewhurst, C.; Russel, C.; Hoell, A.; *J. Non-Cryst. Solids* **2014**, *385*, 24.
- Worch, C.; Buttner, M.; Schaaf, P.; Harizanova, R.; Russel, C.; Schimidt, F.; Seidel, P.; *J. Mater. Sci.* **2013**, *48*, 2299.
- Jungwirth, T.; Nemeč, P.; Novak, V.; *Nat. Photonics* **2013**, *7*, 500.
- Volpi, V.; Montesso, M.; Ribeiro, S. J. L.; Viali, W. R.; Magon, C. J.; Silva, I. D. A.; Donoso, J. P.; Nalin, M.; *J. Non-Cryst. Solids*, *in press*, DOI: 10.1016/j.jnoncrysol.2015.04.022.
- Ravikumar, R. V. S. S. N.; Ikeda, K.; Chandrasekhar, A. V.; Reddy, Y. P.; Rao, P. S.; Yamauchi, J.; *J. Phys. Chem. Solids* **2003**, *64*, 2433.
- Möncke, D.; Kamitsos, E. I.; Herrmann, A.; Ehrt, D.; Friedrich, M.; *J. Non-Cryst. Solids* **2011**, *357*, 2542.
- Srinivasa Reddy, M.; Murali Krishna, G.; Veeraiiah, N.; *J. Phys. Chem. Solids* **2006**, *67*, 789.
- Winterstein-Beckmann, A.; Möncke, D.; Palles, D.; Kamitsos, E. I.; Wondraczek, L.; *J. Non-Cryst. Solids* **2013**, *376*, 165.
- Singh, R. K.; Kothiyal, G. P.; Srinivasan, A.; *J. Non-Cryst. Solids* **2008**, *354*, 3166.
- Singh, S. P.; Chakradhar, R. P. S.; Rao, J. L.; Karmakar, B.; *Phys. B* **2010**, *405*, 2157.
- Ardelean, I.; Toderas, M.; Horea, C.; Filip, S.; *J. Optoelectron. Adv. Mater.* **2008**, *10*, 243.
- Ravi Kumar, A. V.; Srinivasa Rao, Ch.; Narasimha Rao, N.; Ravi Kumar V.; Kityk, I. V.; Veeraiiah, N.; *J. Non-Cryst. Solids* **2012**, *358*, 1278.
- Mogus-Milankovic, A.; Pavic, L.; Srilatha, K.; Rao, Ch. S.; Srikumar, T.; Gandhi, Y.; Veeraiiah, N.; *J. Appl. Phys.* **2012**, *111*, 013714.
- Fuxi, G.; Huimin, L.; *J. Non-Cryst. Solids* **1987**, *95-96*, 61.
- Griscom, D. L.; *J. Non-Cryst. Solids* **1980**, *40*, 211.
- Franco, R. W. A.; Lima, J. F.; Magon, C. J.; Donoso, J. P.; Messaddeq, Y.; *J. Non-Cryst. Solids* **2006**, *352*, 3414.
- Nalin, M.; Messaddeq, Y.; Ribeiro, S. J. L.; Poulain, M.; Briois, V.; Brunklaus, G.; Rosenhahn, C.; Mosel, B. D.; Eckert, H.; *J. Mater. Chem.* **2004**, *14*, 3398.
- Stoll, S.; Schweiger, J.; *Magn. Reson.* **2006**, *178*, 42.
- Gómez, L. A.; de Araújo, C. B.; Messias, D. N.; Misoguti, L.; Zílio, S. C.; Nalin, M.; Messaddeq, Y.; *J. Appl. Phys.* **2006**, *100*, 116105.
- Nalin, M.; Poulain, M.; Poulain, M.; Ribeiro, S. J. L.; Messaddeq, Y.; *J. Non-Cryst. Solids* **2001**, *284*, 110.
- Falcão-Filho, E. L.; de Araújo, C. B.; Bosco, C. A. C.; Maciel, G. S.; Acioli, L. H.; Nalin, M.; Messaddeq, Y.; *J. Appl. Phys.* **2005**, *97*, 013505.
- Kliava, J.; *Phys. Status Solidi B* **1986**, *134*, 411.
- Bogomolova, L. D.; Krasilnikova, N. A.; Bogdanov, V. L.; Khalilev, V. D.; Mitrofanov, V. V.; *J. Non-Cryst. Solids* **1995**, *188*, 130.
- Pascuta, P.; Bosca, M.; Borodi, G.; Culea, E.; *J. Alloys Compd.* **2011**, *509*, 4314.
- Ardelean, I.; Flora, M.; *J. Mater. Sci.* **2002**, *13*, 357.
- Schreurs, J. W. H.; *J. Chem. Phys.* **1978**, *69*, 2151.
- Abraham, A.; Bleaney, B.; *Electron Paramagnetic Resonance of Transition Ions*; Oxford University Press: Oxford, 1970.
- Priya, V. V.; Upender, G.; Prasad, M.; *Glass Phys. Chem.* **2014**, *40*, 144.
- Kripal, R.; Maurya, M.; *Mater. Chem. Phys.* **2008**, *108*, 257.
- Singh, R. K.; Srinivasan, A.; *J. Magn. Mater.* **2010**, *322*, 2018.
- Muralidhara, R. S.; Kesavulu, C. R.; Rao, J. L.; Anavekar, R. V.; Chakradhar, R. P. S.; *J. Phys. Chem. Solids* **2010**, *71*, 1651.
- Ardelean, I.; Cora, S.; Lucacel, R. C.; Hulpus, O.; *Solid State Sci.* **2005**, *7*, 1438.
- Cerný, V.; Petrova, B.; Frumar, M.; *J. Non-Cryst. Solids* **1990**, *125*, 17.
- Toloman, D.; Giurgiu, L. M.; Ardelean, I.; *Phys. B* **2009**, *404*, 4198.
- Konidakis, I.; Varsamis, C. E.; Kamitsos, E. I.; Moncke, D.; Ehrt, D.; *J. Phys. Chem. C* **2010**, *114*, 9125.
- Winterstein, A.; Akamatsu, H.; Moncke, D.; Tanaka, K.; Shimidt, M. A.; Wondraczek, L.; *Opt. Mater. Express* **2013**, *48*, 2299.

42. Kawano, M.; Takebe, H.; Kuwabara, M.; *Opt. Mater.* **2009**, *32*, 277.
43. Molla, A. R.; Chakradhar, R. P. S.; Kesavulu, C. R.; Rao, J. L.; Biswas, S. K.; *J. Alloys Compd.* **2012**, *512*, 105.
44. Kiran, N.; Kesavulu, C. R.; Kumar, A. S.; Rao, J. L.; *Phys. B* **2011**, *406*, 3816.
45. Reisfeld, R.; Kisilev, A.; Jorgensen, C. K.; *Chem. Phys. Lett.* **1984**, *111*, 19.
46. Li, P.; Peng, M.; Wondraczek, L.; Zhao, Y.; Viana, B.; *J. Mater. Chem. C* **2015**, *3*, 3406.

Submitted: July 20, 2015

Published online: October 30, 2015

**FAPESP has sponsored the publication of this article.**